Supplementary Information for: Theoretical exploration of MgH$_2$ and graphene nano-flake in cyclohexane: proposing a new perspective toward functional hydrogen storage material

Runze Liu,[a,d]   Yinghe Zhao[b,d] and Tianshu Chu[*a,c]

[a] State Key Laboratory of Molecular Reaction Dynamics, Dalian Institute of Chemical Physics, Chinese Academic of Sciences, Dalian 116023, P. R. China.

[b] Institute of Theoretical Chemistry, Jilin University, Changchun 130012, P. R. China.

[c] Institute for Computational Sciences and Engineering, Laboratory of New Fiber Materials and Modern Textile, The Growing Base for State Key Laboratory, Qingdao University, Qingdao 266071, China. E-mail: tschu@dicp.ac.cn; tschu008@163.com

[d] These authors contributed equally to this work.

Computation details:

All quantum mechanism (QM) calculations are carried out using the GAUSSIAN 09 program package [1]. The transition states are calculated by applying firstly synchronous transit guided quasi-Newton method [2, 3] to orient an approximately reasonable conformation and then Berny algorithm [4] to determine the final conformation. Intrinsic reaction coordinate calculations [5-7] are also performed to ensure that the transition states indeed bridge the reactants and products. These are calculated at the B3LYP/6–311+G* level of theory [8-13] that has proven rational on Mg$_m$C$_n$H$_x$ cluster research [14]. Intermolecular interaction is calculated at the B3PW91/6–31 level of theory [9, 15] with basis set superposition error correction [16, 17] and DFT-D3 (BJ-damping) method [18, 19]. We compare the energy values obtained by three different DFT methods (B3PW91/6–31G, B3LYP/6–31G and B3LYP/6-31G(d,p)). The corresponding results (Table S1) are accordant for the calculation of intermolecular interaction, and the latter method has been verified to be good enough for the description of Mg^{2+} [20]. As a result, B3PW91/6–31G can precisely mimic the trend of intermolecular interaction in terms of the system reported in the present work.

Table S1. The single point energy values of cyclohexane/magnesium hydride with graphene nano-flake in two typical distances (see Fig. 2) given by three different DFT methods.

cyclohexane		B3PW91/6-31G	B3LYP/6-31G	B3LYP/6-31G(d,p)
E1$_{(r=0.4 nm)}$	hartree	-4290.701209181704	-4292.239777 015363	-4293.301639652918
E2$_{(r=2.0 nm)}$	hartree	-4290.686454448875	-4292.226132894762	-4293.287802337632
E2-E1	kJ/mol	**38.393278**	**35.838490**	**36.345947**
magnesium hydride		B3PW91/6-31	B3LYP/6-31	B3LYP/6-31G(d,p)
E1$_{(r=0.31 nm)}$	hartree	-4256.117457778788	-4257.630726045846	-4258.625524290096
E2$_{(r=2.00 nm)}$	hartree	-4256.105075789665	-4257.620576981172	-4258.614167054452
E2-E1	kJ/mol	**32.523301**	**26.658160**	**29.813617**

All simulations are performed under the condition of berendsen barostat at 3 MPa and thermostat at 500 K as the experiment reported [21]. The leapfrog integration algorithm is applied and the time step is set to 1 fs. The

electrostatic and Lennard-Jones interactions inside 1 nm are calculated with direct coulomb law and 12-6 type. They outside 1 nm are considered using the Smoothed Particle Mesh Ewald sum [22] and cut respectively. The atomic point charge evaluation depends on the chelpg methodology [23] at the B3LYP/6–311+G* level of theory [8-13] and is calculated using GAUSSIAN 09 program package [1]. The intermolecular interaction between magnesium hydride and graphene nano-flake is determined by fitting the QM result (see the red solid line in Fig. 2). The other force field parameters are all obtained from amber99sb [24] by using AnteChamber PYthon Parser interface [25, 26]. We constructed 9 different systems:

(I)   *200 n-butane molecules (Fig. S1b) in 4716 cyclohexane molecules (Fig. S1a);*

(II)   *200 1-butene molecules (Fig. S1c) in 4798 cyclohexane molecules;*

(III)   *250 magnesium hydride (Fig. S1d) molecules in 4735 cyclohexane molecules;*

(IV)   *200 butyl(hydride) magnesium (Fig. S1e) molecules in 4622 cyclohexane molecules;*

(V)   *250 magnesium hydride molecules and 1 graphene nano-flake (Fig. S3a) in 4735 cyclohexane molecules;*

(VI)   *(a) 150 magnesium hydride molecules and 1 graphene nano-flake (Fig. S3a) in 4943 cyclohexane molecules; (b) 150 magnesium hydride molecules in 4943 cyclohexane molecules;*

(VII)   *(a) 350 magnesium hydride molecules and 1 graphene nano-flake (Fig. S3a) in 4552 cyclohexane molecules; (b) 350 magnesium hydride molecules in 4552 cyclohexane molecules;*

(VIII)   *(a) 250 magnesium hydride molecules and 1 graphene nano-flake (Fig. S3b) in 4735 cyclohexane molecules; (b) 250 magnesium hydride molecules in 4735 cyclohexane molecules;*

(IX)   *(a) 250 magnesium hydride molecules and 1 graphene nano-flake (Fig. S3c) in 4622 cyclohexane molecules; (b) 250 magnesium hydride molecules in 4622 cyclohexane molecules;*

The systems without graphene nano-flake are carried out with Gromacs-4.5.5 [27], and the system with graphene nano-flake are performed using DL_POLY_4.06 [28]. The position of graphene nano-fake is maintained frozen all the time.
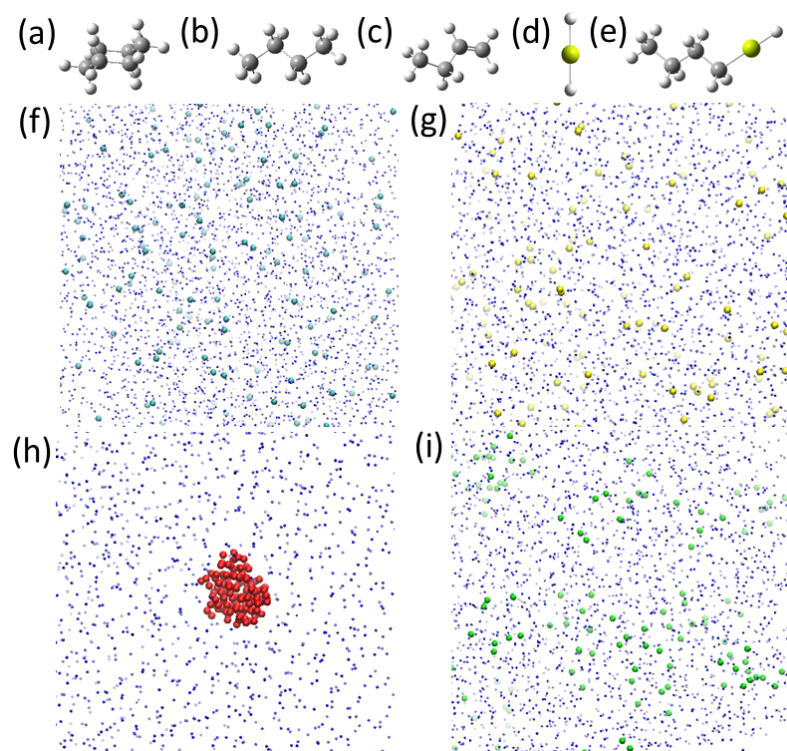
Fig. S1 (a), (b), (c), (d) and (e) are geometry optimized structures of cyclohexane, n-butane, 1-butene, magnesium hydride amd butyl(hydride) magnesium respectively. (f), (g), (h) and (i) depict the states of n-butane (b), 1-butene (c), magnesium hydride (d) and butyl(hydride) magnesium (e) in cyclohexane (a). To get better visualization effect, we use the gray ball, yellow ball, red ball, green ball and blue point to represent (b), (c), (d), (e) and (a). These four configurations correspond to the systems (I), (II), (III) and (IV) after equilibrium (described in computation details), and they are captured by VMD [29].
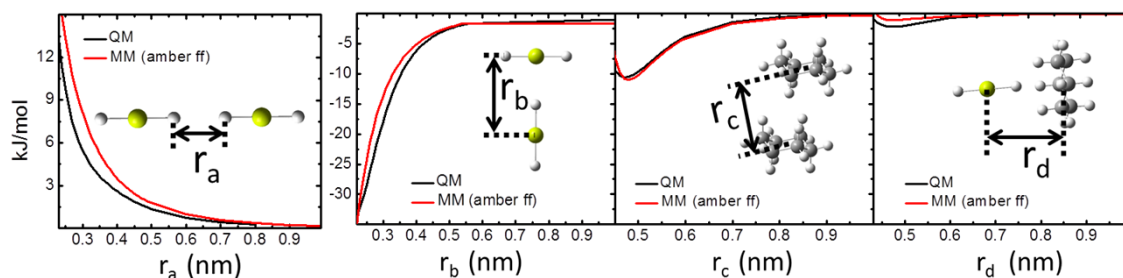
Fig. S2 Black and red lines record the intermolecular interactions calculated with QM and MM (amber force field) methods when scanning r_a, r_b, r_c and r_d. The given placements are typical configurations in which the molecular interactions are considerably stronger compared with other arrangements.
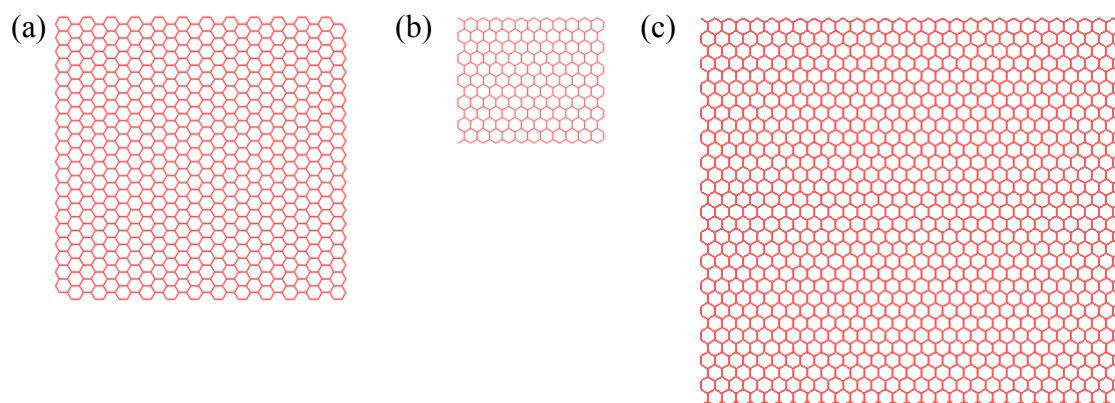
Fig. S3 The structures of graphene nano-flakes in MD simulations. Their sizes are approximately 5.2 nm × 5.2 nm, 3.0 nm × 2.5 nm and 7.4 nm × 6.8 nm, respectively.
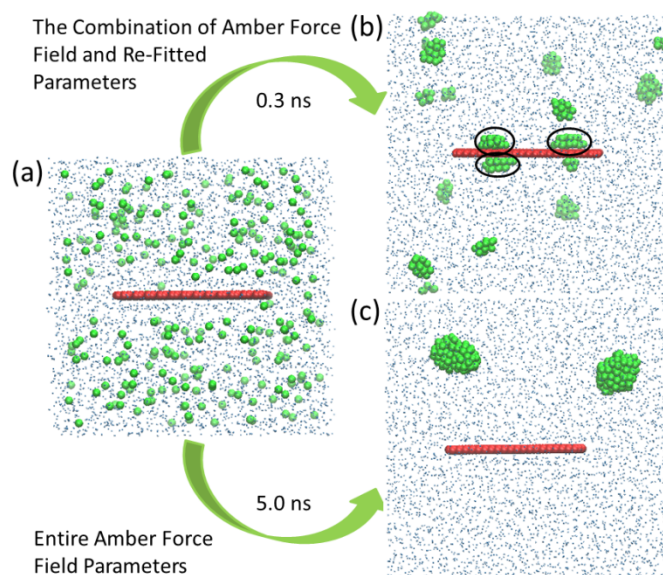
Fig. S4 (a) records the initial configuration of system V in computation details. (b) and (c) are the dynamic evolutions of (a) at t = 0.3 ns and 5.0 ns with two different force fields, i.e., the combination of amber force field and re-fitted parameters as well as entire amber force field. The plate, ball and point represent graphene nano-flake, MgH_2 and cyclohexane respectively. These three configurations are obtained using VMD [29].

A   (150 MgH₂ molecule and 5.2 nm × 5.2 nm graphene nano-flake)
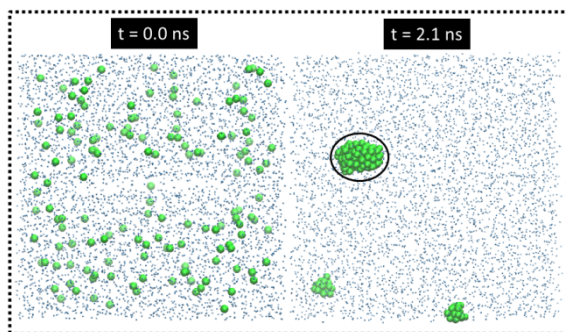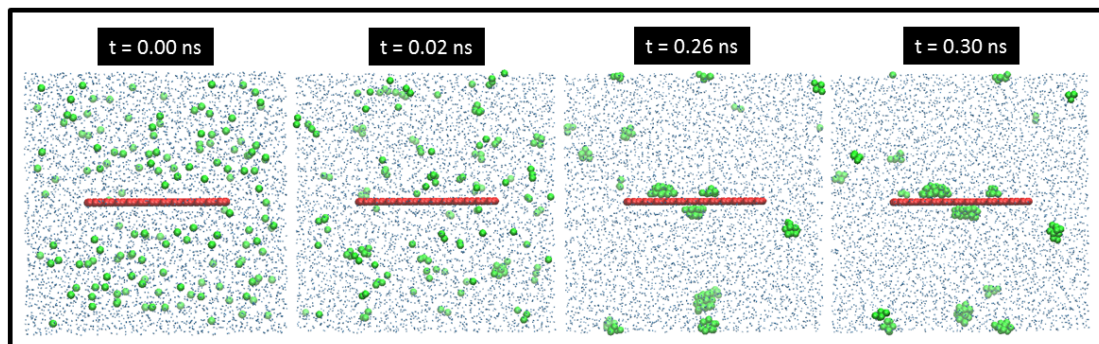
B   (350 MgH₂ molecule and 5.2 nm × 5.2 nm graphene nano-flake)
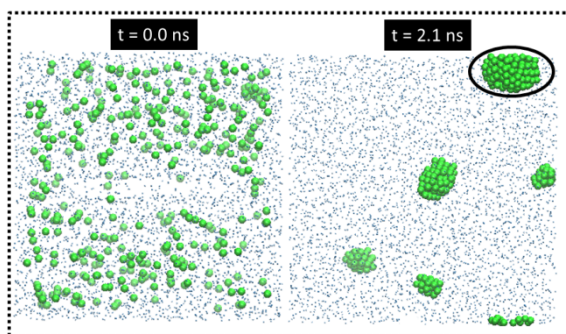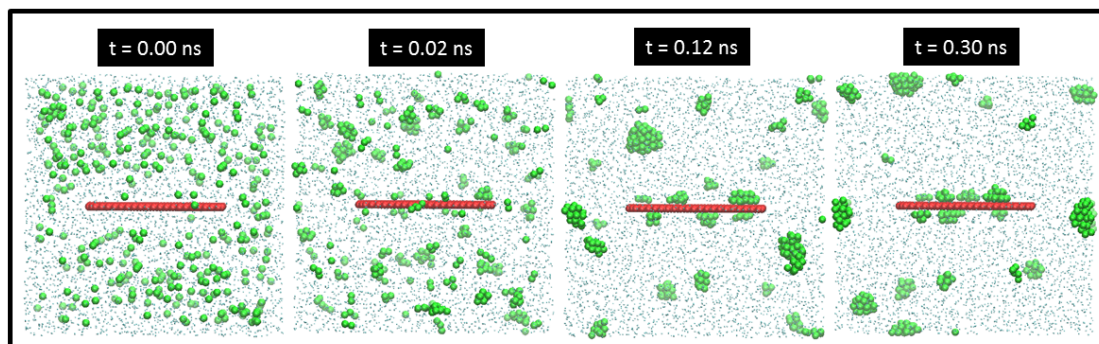
C   (250 MgH₂ molecule and 3.0 nm × 2.5 nm graphene nano-flake)
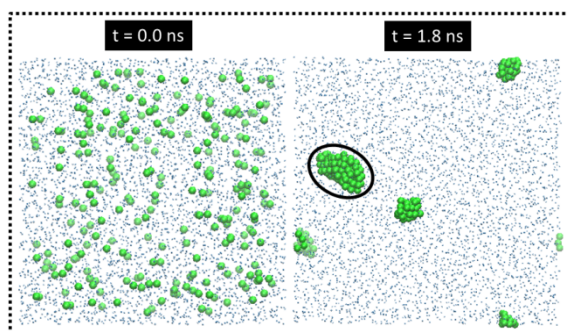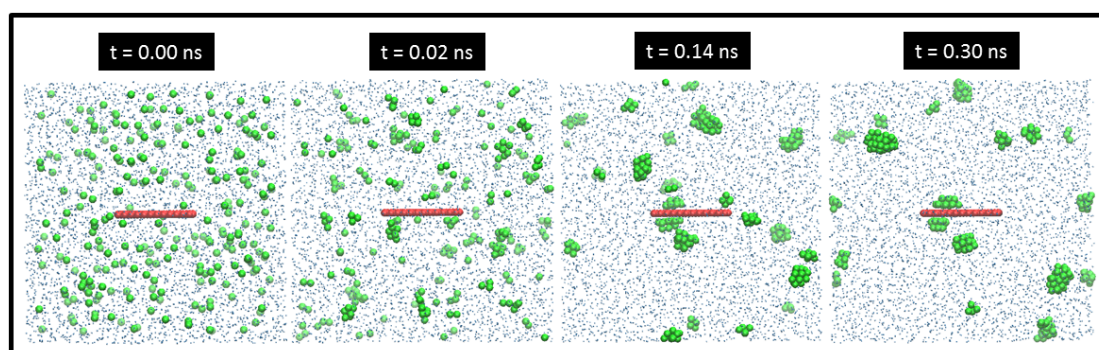
D   **(250 MgH₂ molecule and 7.4 nm × 6.8 nm graphene nano-flake)**
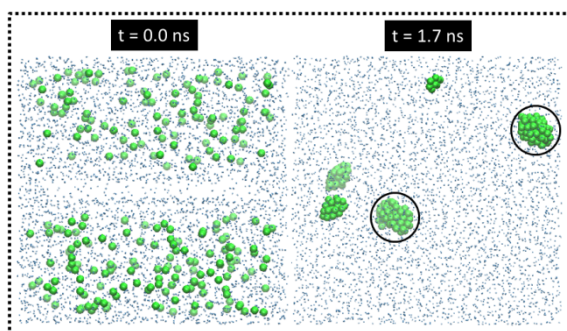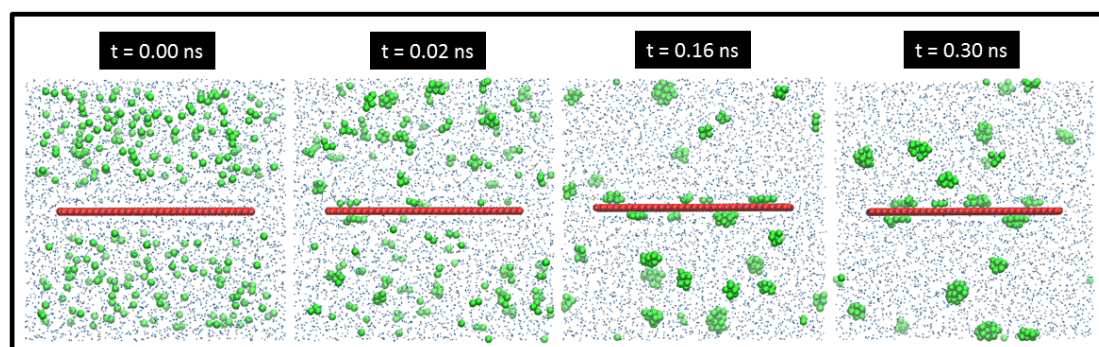
Fig. S5 A-D represent systems VI-IX in computation details. Herein the configurations surrounded by solid and dotted lines correspond to the (a) and (b) of systems VI-IX, respectively. The configurations at t = 0.0 ns are the initial configurations, and the others are the corresponding dynamic evolutions at different times. It is noteworthy that the clusters circled by circular or oval frames are ones that just form and outweigh others in size. Graphene nano-flake, MgH₂ and cyclohexane are displayed by the plate, ball and point, respectively. All configurations are captured using VMD [29].

1   M. J. Frisch, G. W. Trucks, H. B. Schlegel et al., GAUSSIAN 09, Revision D.01, Gaussian, Inc., Wallingford, CT, 2009

2   C. Peng and H. B. Schlegel, *Israel J. Chem.*, 1993, *33*, 449.

3   C. Peng, P. Y. Ayala, H. B. Schlegel and M. J. Frisch, *J. Comp. Chem.*, 1996, *17*, 49.

4   X. Li and M. J. Frisch, *J. Chem. Theory and Comput.*, 2006, **2**, 835.

5   C. Gonzalez and H. B. Schlegel, *J. Phys. Chem.*, 1990, **94**, 5523.

6   C. Gonzalez and H. B. Schlegel, *J. Chem. Phys.*, 1989, **90**, 2154.

7   D. G. Truhlar and M. S. Gordon, *Science*, 1990, **249**, 491.

8   A. D. Becke, *J. Chem. Phys.*, 1993, **98**, 5648.

9   C. Lee, W. Yang and R. G. Parr, *Phys. Rev. B*, 1988, **37**, 785.

10   B. Miehlich, A. Savin, H. Stoll and H. Preuss, *Chem. Phys. Lett.*, 1989, **157**, 200.

11   A. D. McLean and G. S. Chandler, *J. Chem. Phys.*, 1980, **72**, 5639.

12   T. Clark, J. Chandrasekhar, G. W. Spitznagel and P. V. R. Schleyer, *J. Comput. Chem.*, 1983, **4**, 294.

13   M. J. Frisch, J. A. Pople and J. S. Binkley, *J. Chem. Phys.*, 1984, **80**, 3265.

14   F. Dong, Y. Xie and E. R. Bernstein, *J. Chem. Phys.*, 2011, **135**, 054307.

15   J. P. Perdew and Y. Wang, *Phys. Rev. B*, 1992, **45**, 13244.

16   S. F. Boys and F. Bernardi, *Mol. Phys.*, 1970, **19**, 553.

17   S. Simon, M. Duran and J. J. Dannenberg, *J. Chem. Phys.*, 1996, **105**, 11024.

18   S. Grimme, J. Antony, S. Ehrlich and H. Krieg, *J. Chem. Phys.*, **132**, 154104 2010.

19   S. Grimme, S. Ehrlich and L. Goerigk, *J. Comput. Chem.*, 2011, **32**, 1456.

20   R. A. Torres, F. Himo, T. C. Bruice, L. Noodleman and T. Lovell, *J. Am. Chem. Soc.*, 2003, **125**, 9861.

21   E. J. Setijadi, C. Boyer and K. F. Aguey-Zinsou, *Int. J. Hydrogen Energy*, 2013, **38**, 5746.

22   U. Essmann, L. Perera, M. L. Berkowitz, T. Darden, Hs. Lee and L. G. Pedersen, *J. Chem. Phys.*, 1995, **103**, 8577.

23   C. M. Breneman and K. B. Wiberg, *J. Comput. Chem.*, 1990, **11**, 361.

24   A. T. Guy, T. J. Piggot and S. Khalid, *Biophysical Journal*, 2012, 103, 1028.

25   J. Wang, W. Wang, P. A. Kollman and D. A. Case, *J. Mol. Graphics Model*, 2006, **25**, 247.

26   A. Sousa da Silva and W. Vranken, *BMC Research Notes*, 2012, **5**, 367.

27   B. Hess, C. Kutzner, D. Van der Spoel, E. Lindahl, *J. Chem. Theory Comput.*, 2008, **4**, 435.

28   I. T. Todorov, W. Smith, K. Trachenko and M. T. Dove, *J. Mater. Chem.*, 2006, **16**, 1911.

29   W. Humphrey and A. Dalke, K. Schulten, J. Mol. Graphics, 1996, **14**, 33.